J. Membrane Biol. 90, 177–190 (1986)

The Journal of
Membrane Biology

Ionic Channels Formed by *Staphylococcus aureus* Alpha-Toxin: Voltage-Dependent Inhibition by Divalent and Trivalent Cations

Gianfranco Menestrina
Dipartimento di Fisica, Università di Trento, 38050 Povo (TN), Italy

Summary. The interaction of *Staphylococcus aureus* α-toxin with planar lipid membranes results in the formation of ionic channels whose conductance can be directly measured in voltage-clamp experiments. Single-channel conductance depends linearly on the solution conductivity suggesting that the pores are filled with aqueous solution; a rough diameter of 11.4 ± 0.4 Å can be estimated for the pore. The conductance depends asymmetrically on voltage and it is slightly anion selective at pH 7.0, which implies that the channels are asymmetrically oriented into the bilayer and that ion motion is restricted at least in a region of the pore. The pores are usually open in a KCl solution but undergo a dose- and voltage-dependent inactivation in the presence of di- and trivalent cations, which is mediated by open-closed fluctuations at the single-channel level. Hill plots indicate that each channel can bind two to three inactivating cations. The inhibiting efficiency follows the sequence $Zn^{2+} > Tb^{3+} > Ca^{2+} > Mg^{2+} > Ba^{2+}$, suggesting that carboxyl groups of the protein may be involved in the binding step. A voltage-gated inactivation mechanism is proposed which involves the binding of two polyvalent cations to the channel, one in the open and one in the closed configuration, and which can explain voltage, dose and time dependence of the inactivation.

Key Words *Staphylococcus aureus* · α-toxin · ionic channel · voltage gating · divalent cations · inactivation · selectivity · planar lipid membranes

Introduction

Staphylococcus aureus α-toxin is a cytolytic exotoxin whose main component is a single water-soluble polypeptide with a molecular weight of 34,000 daltons [19, 21]. The polypeptide is strongly surface active being able either to insert into preformed lipid monolayers increasing their surface pressure [11, 19], and to form itself monolayers at an air-water interface [11], suggesting the presence of a hydrophobic region in it. This protein also has strong membrane-damaging properties and causes erythrocyte lysis via three stages: (i) binding of the toxin to the cell membrane, (ii) K^+-ion leakage and (iii) hemoglobin release [12, 23]. The molecular events leading to membrane damage are not yet completely understood though it has been proposed that native α-toxin oligomerizes on the membrane to form an amphiphilic hexameric complex that, through its partial embedment within the lipid bilayer, generates a transmembrane channel responsible for ion leakage [1, 5, 19, 20, 21, 39]. Attacked membranes show in fact under the electron microscope typical lesions which appear as 10-nm diameter annular structures harboring a 2 to 3-nm central pool of stain which may be related to the ion pathway [19, 21]. A colloid-osmotic shock is thought to follow the leakage of ions, leading to the lysis of the membrane and ultimately to the death of the cell.

To shed some further light on the mechanism of this interaction we have studied the effects of *S. aureus* α-toxin on planar lipid membranes comprised of phospholipids. We have found that this toxin forms ionic channels of well-defined conductance either in neutral membranes comprised of pure phosphatidylcholine or in negatively charged bilayers containing phosphatidylserine.

Pasternak and coworkers have recently shown that α-toxin damage to intact cells can be prevented by extracellular Ca^{2+} as well as by other divalent cations, and they have proposed that this protection mechanism can be physiologically relevant [2, 35]. Similar results have been presented also by Harshman and Sugg [24]. For this reason we have studied the effects of di- and trivalent cations on the conductance induced by α-toxin in planar bilayers in detail. We have found that polyvalent cations produce a dose- and voltage-dependent closure of the α-toxin channels by specifically binding to them, the sequence of inhibiting potency being $Zn^{2+} > Tb^{3+} > Ca^{2+} > Mg^{2+} > Ba^{2+}$.

This is the same sequence which has been found to hold also for intact cells [2, 35], suggesting that the protection against toxin damage operated by divalent cations occurs via the closing of pre-

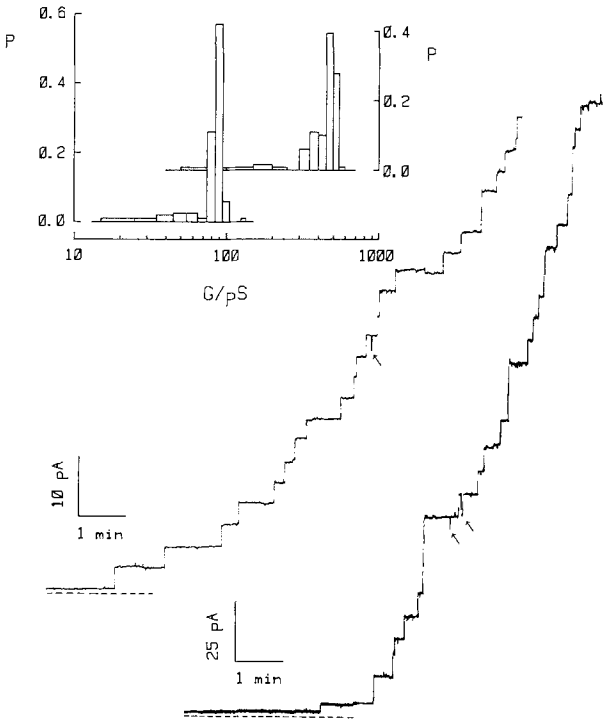

Fig. 1. Current steps after the addition of *S. aureus* α-toxin to one side of a PC planar bilayer clamped at +40 mV; each one is due to the opening of a new ionic channel into the membrane. Upper trace: KCl 0.1 M, α-toxin 10 μg/ml; lower trace KCl 0.5 M, α-toxin 5μg/ml. Dashed lines indicate zero current while arrows point at occasional fluctuations of channels to a closed state. Insert: cumulative histograms representing the probability *P* to observe a step of a given conductance during experiments like those in the lower traces. Due to the large variation of the channel conductance a logarithmic scale has been used for the abscissa. Experimental conditions are: lower histogram, 114 steps from two different experiments with KCl 0.1 M, bin width 10 pS, left vertical scale; upper histogram, 119 steps from three different experiments with KCl 0.5 M, bin width 50 pS, right vertical scale. In common: clamp voltage +40 mV, planar bilayers comprised of egg PC

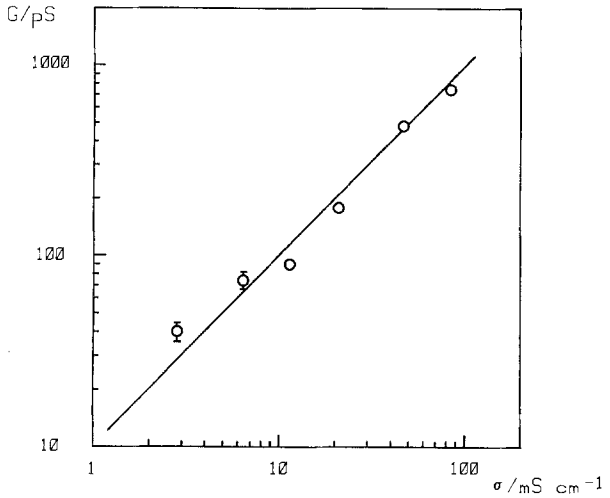

Fig. 2. α-toxin channel conductance as a function of the conductivity of the solution for KCl concentrations ranging from 0.02 to 1 M. Conductance values are obtained from incorporation traces like those shown in Fig. 1 and are the mean from a minimum of two up to eight different experiments at the same concentration. More than 650 steps were evaluated to build up the figure; error bars exceeding the point widths are reported. Solid line is a least-squares adaptation of a straight line with slope +1. The intercept is found to be 10.1 ± 1.0 × 10^{-9} cm (mean ± SD). Other conditions as in Fig. 1

formed channels by a specific binding of these inactivating cations and not by preventing the formation of channels. Closure of the channels can indeed impede the colloid-osmotic shock of the cells giving them the opportunity to repair their lesions [35].

We conclude that the early stage of membrane lysis by α-toxin is the formation of an ionic channel of well-defined size which can be made to close by divalent cations.

Materials and Methods

Planar phospholipid bilayer membranes were prepared at room temperature by the apposition of two monolayers with the Montal technique [34]. Lipids used were either reduced egg phosphatidylcholine alone (PC, by P-L-Biochemicals, more than 99% pure) or a mixture of the same lipid with bovine brain phosphatidylserine (PS, by Calbiochem) in a molar ratio 1 : 1. Monolayers were spread from a 5 mg/ml solution of these lipids in *n*-hexane and after evaporation of the solvent membranes were formed on a hole in a 12-μm thick Teflon septum separating two buffered salt solutions. The hole had a diameter of about 0.2 mm and was pretreated with a 1 : 20 solution of hexadecane in hexane. Bathing solutions, 4 ml on each side, contained various amounts of KCl or $CaCl_2$, as specified in the text, 1 mM EDTA (Merck) and were buffered by 10 mM Tris (Calbiochem) at pH 7.0 if not otherwise stated. The conductivity of each buffer solution has been measured with a Philips PW9509 digital conductimeter equipped with a PW9514 cell (cell constant 1 cm^{-1}). Di- and trivalent cations were added either to one or to both solutions during the experiment, and the addition was followed by a vigorous mixing of the solutions with magnetic bars; the concentrations given in the text are corrected for the presence of EDTA.

Staphylococcus aureus α-toxin was a kind gift of Dr. K.D. Hungerer of the Behringwerke laboratories (Marburg, D). It has been shown by chromatography over Sephacryl S-300 that this preparate contains 75% of protein eluting in a sharp symmetrical peak of mol wt 30 to 40 kD corresponding to α-toxin in monomeric form and 25% eluting in a second peak in the mol wt region 180 to 500 kD corresponding to larger toxin aggregates [5]. α-toxin from stock aqueous solution was added, after the membrane was completely formed and stabilized, to one compartment only (*cis* side) to a final concentration ranging from 5 to 30 μg/ml, i.e. in the same concentration range in which it has been shown to induce permeabilization of erythrocytes as well as non-erythroid cells and multilamellar liposomes [2, 18–21, 35]. By means of two Ag–AgCl electrodes, connected to the solution

through agarose bridges saturated with 3 M KCl, the transmembrane potential was clamped to the desired value and the current sent to an *I–V* converter built around a virtual grounded operational amplifier (Burr Brown OPA 104 C) with feedback resistors ranging from 10^6 to 10^8 Ω. *Cis* compartment was connected to the virtual ground and voltage signs are referred to it; current is defined as positive when cations flow into this compartment.

Results

α-Toxin Forms Ionic Channels into Planar Bilayer Membranes

The addition of small amounts of *S. aureus* α-toxin to the solution bathing a planar bilayer yields, under voltage-clamp conditions, a stepwise increase of the current flowing through the membrane (Fig. 1). The current steps are rather homogeneous in size and, as can be seen comparing the two traces shown, which have been obtained with different KCl concentrations, their amplitude depends on the salt activity in the bathing solution. From the height of each jump a conductance value for the unitary event can be calculated and from incorporation traces like those shown in Fig. 1 cumulative histograms representing the probability of observing a jump of a given conductance can be constructed. This is done in the insert of Fig. 1 for the experimental conditions of the two traces shown below. Though the distribution is asymmetrical (there is in fact an excess of events with low conductance) the great majority of events fall under a well-pronounced peak whose large conductance value (about 90 pS at 0.1 M KCl and 450 pS at 0.5 M) indicates that this protein increases the conductance of the bilayer by opening ionic channels through it.

The mean conductance of the α-toxin channel is shown in Fig. 2 as a function of the conductivity of the electrolyte solution for different KCl concentrations and a constant clamp voltage of +40 mV. The straight line through the points has a slope of 1 which indicates a linear relationship between the two variables. Despite the simple relation between channel conductance and solution conductivity the α-toxin channel shows a voltage-dependent instantaneous conductance. This is shown in Fig. 3 where a current-voltage curve obtained applying short-lived voltage pulses (duration about 0.5 sec) to a membrane containing many α-toxin channels bathed by 0.1 M KCl is reported (full points). The curve has been normalized by dividing it by the factor which gives at +40 mV the mean current measured for the single channel during the initial incorporation. Such a curve is nonlinear: it increases

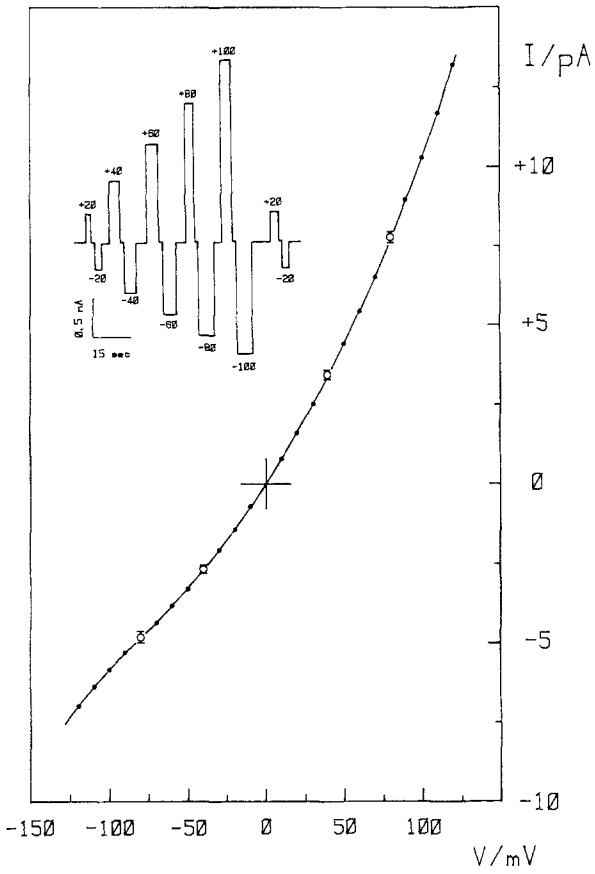

Fig. 3. Current-voltage characteristic of α-toxin channels in PC bilayers bathed by 0.1 M KC. Full points are from instantaneous current-voltage curves obtained on membranes containing many channels: seven curves from three different experiments have been normalized to the mean current flowing through a single channel at +40 mV and then averaged to give the experimental points. Open circles are mean single-channel values obtained from incorporation traces like those in Fig. 1, recorded at different clamping voltages (a total of 302 steps from 12 different experiments have been used). Solid line is drawn by eye. Insert: Current response to the application of long-lasting voltage pulses to a membrane containing many α-toxin channels (roughly 200). Voltage pulses were from a 0-mV holding potential to the final potential indicated in mV in the figure on top of each current pulse. Other conditions as above

overlinearly in the first quadrant and sublinearly in the third. That this is indeed a property of the single channel is shown by the comparison of this curve with the mean channel conductance obtained at different clamp voltages by cumulative histograms like those shown in the insert of Fig. 1, which are reported in Fig. 3 as open circles. Finally the upper insert of Fig. 3 indicates that also applying long-lasting voltage pulses, with durations of many seconds, to a membrane containing many channels the current-voltage curve is nonlinear and there is no time dependence once the voltage is constant. Simi-

Table 1. Ion selectivity of the *S. aureus* α-toxin channel[a]

Salt	pH	c/M	c'/M	f	f'	V_{rev}/mV	t_a/t_c
KCl	7.0	0.5	0.1	.66	.80	−7.3 ± 1.5	1.52 ± 0.14
KCl	7.0	0.5	0.05	.66	.87	−10.8 ± 0.2	1.54 ± 0.03
KCl	5.0	1.0	0.1	.62	.80	−20.1 ± 0.9	2.29 ± 0.10
$CaCl_2$	7.0	0.05	0.01	.59	.75	−17.5 ± 0.6	2.07 ± 0.11

[a] Reversal potentials have been measured in a KCl or $CaCl_2$ gradient at the pH indicated. c and c' are the concentrations in the *cis* and *trans* compartment, respectively, whereas f and f' are the activity coefficients in the two compartments calculated according to [36]. V_{rev} is the zero-current potential developed in the *trans* compartment. The ratio between anion transport number t_a, and cation transport number t_c, has been calculated from Eq. (3) in the text.

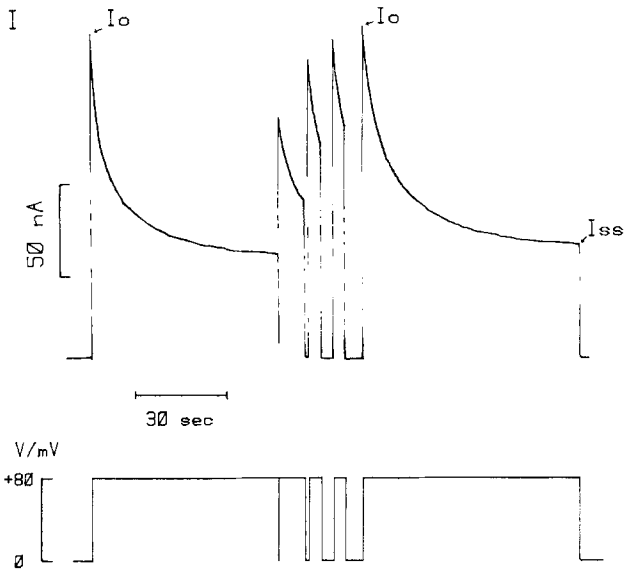

Fig. 4. Time course of current after the application of voltage pulses of +80 mV to a PC : PS membrane (molar ratio 1 : 1) containing many α-toxin channels in the presence of 4 mM $CaCl_2$ added to a 0.1 M KCl solution after the channels were already formed. The pulse protocol is shown in the lower part of the figure. After reaching a large instantaneous value *Io* at the time of the jump to the high voltage, the current then relaxes to a lower steady-state value *Iss*. A permanence at 0 mV can reestablish the high conductance level only if it is long enough, as evidenced by successive jumps at 0 mV of increasing duration. α-toxin concentration here was 25 μg/ml

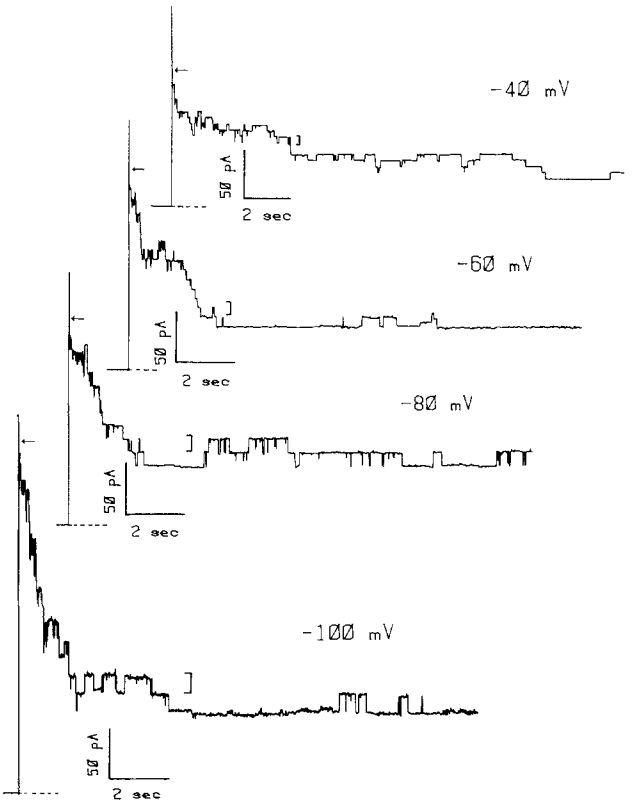

Fig. 5. Time course of current after the application of voltage pulses from a 0-mV holding potential to a PC membrane containing about 20 α-toxin channels. Bathing solutions were 0.1 M KCl plus 40 mM $CaCl_2$; α-toxin was 5 μg/ml. Discrete current fluctuations of about 160 pS are evident in these conditions. Applied voltages are indicated on each trace. Vertical bars indicate a conductance of 200 pS; current and time scales are 50 pA and 2 sec in all four traces. Dashed lines indicate zero of current. The initial fast transient, indicated by arrows, is due to the charging of the membrane capacity

lar results have been obtained also using bathing solutions containing 0.2 and 0.5 M KCl.

To further investigate the mechanism of ion transport through the channel we have performed reversal potential experiments, i.e. we have measured the potential at which the current flowing through a membrane containing many α-toxin channels and separating two asymmetrical KCl or $CaCl_2$ solutions becomes zero. The results of these experiments are shown in Table 1. We have found that if the *cis* compartment is made the more concentrated then the potential of the *trans* compartment becomes negative in conditions of no net current flowing. This finding implies that the channels are preferentially permeable to the anions, but the small absolute value measured indicates that cations also can pass through the channel to a certain extent. The selectivity of the channel depends on the pH of the solution; in fact, as shown in Table 1, reducing the pH from 7.0 to 5.0 roughly doubles the reversal potential in a tenfold KCl concentration gradient, i.e. it increases the anion selectivity of the α-toxin channel.

Divalent Cations Close the α-Toxin Channels

As shown by Pasternak et al. [35] and Harshman and Sugg [24] the permeabilizing effects of α-toxin

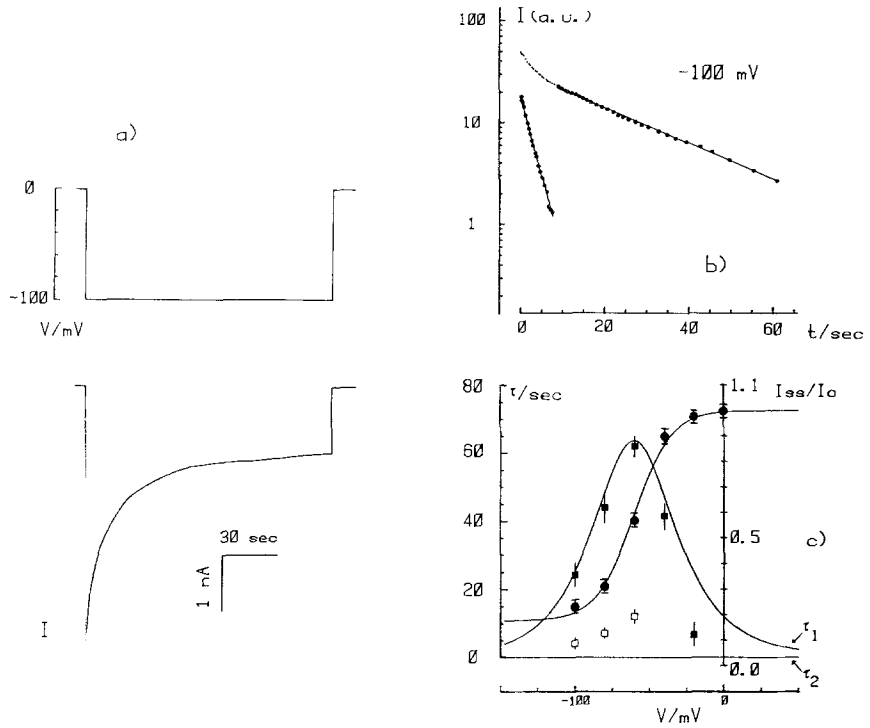

Fig. 6. Voltage and time dependence of the α-toxin induced conductance in a PC bilayer bathed by 0.1 M KCl plus 60 mM $CaCl_2$ only in the *trans* compartment. *a*) Current relaxation like those of Figs. 4 and 5 at −100 mV. *b*) Digitized time course of the current, measured in arbitrary units, after a step transition from 0 to −100 mV plotted on a half-logarithmic scale (upper trace). Solid line is the least-squares fit to the enlarged points which gives a time constant τ_1 = 62 sec. The lower trace is the residual current after the subtraction of the exponential relaxation of time constant τ_1. A second regression line can be calculated from these points which gives a second time constant τ_2 = 12 sec. *c*) Voltage dependence of the ratio *Iss/Io*, full circles and right vertical scale, and of the two time constants τ_1 and τ_2, full and open squares, respectively (left vertical scale). Results from three relaxations like those in part *a*) for each value of the final voltage have been averaged. Solid lines are drawn according to the inactivation model described in the text with the parameters reported in Table 2

on whole cells can be inhibited by Ca^{2+} and other divalent cations. To clarify this aspect of the α-toxin channel properties we have studied the effects of divalent cations on preformed channels in detail. Figure 4 exemplifies the action of 5 mM Ca^{2+} added symmetrically to the 0.1 M KCl solutions bathing a PC/PS membrane containing many α-toxin channels. In contrast to what we have shown in the insert of Fig. 3, the current flowing through the membrane after application of a voltage jump becomes strongly time dependent when divalent cations are present in the solution. On a step transition of the clamp voltage from 0 to +80 mV the current shows a large initial value *Io* which then rapidly decreases in an exponential-like manner towards a lower steady-state value *Iss*. Reverting the potential to 0 mV releases this inhibition of the α-toxin-induced conductance; the extent of the relief is larger the longer the time spent at 0 mV. In the experimental conditions of Fig. 4 a 6-sec period at 0 mV is sufficient for a complete relief of the inhibiting effects of a +80 mV voltage step.

The elementary events leading to this decrease can be better understood looking at Fig. 5. Here from a 0-mV resting potential, voltage steps of increasing amplitudes have been applied to a PC membrane containing few α-toxin channels, in the presence of Ca^{2+}. Also in this case the current, starting from a maximum at the time of the voltage change, which corresponds to all the channels being open, decreases then in discrete steps each representing the closure of one individual channel. Both the amplitude of the relaxation and its decaying rate are larger the larger the applied potential.

The voltage and time dependence of the inhibiting effects of Ca^{2+} are studied in detail in Fig. 6 for the case of a PC membrane containing many α-toxin channels bathed by symmetrical 0.1 M KCl plus 60 mM $CaCl_2$ on the *trans* side. An example of current transient after the application of a voltage step from a holding potential of 0 mV, is shown in part *a*. The extent of the inhibition, i.e. the amplitude of the current relaxation, is larger the larger the applied potential; this is made evident in part *c* where the ratio *Iss/Io* is reported as a function of the final voltage; it can be seen that this ratio decreases sigmoidally when the applied potential is increased. The time course of the transient to −100 mV is

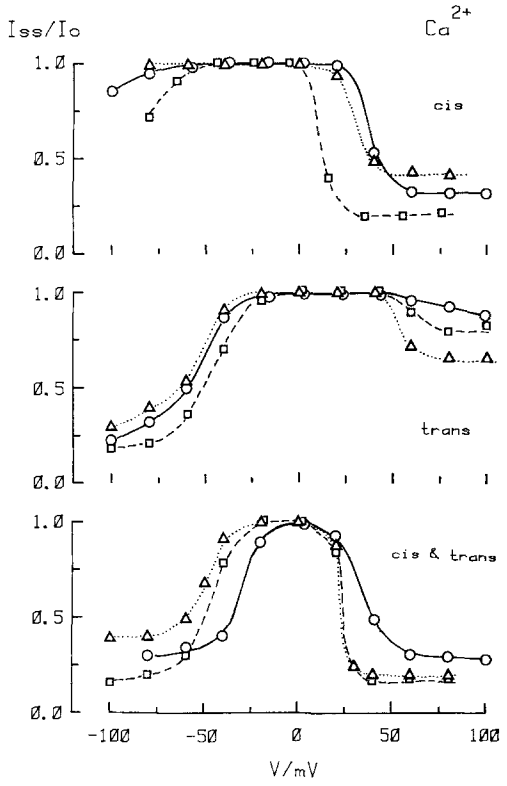

Fig. 7. Sidedness of the inhibiting action of Ca^{2+} on the α-toxin-induced conductance in PC bilayers. 50 mM $CaCl_2$ have been added either on the *cis* side of the membrane (upper panel) or on the *trans* side (middle panel), or on both sides (lower panel). KCl concentration was either 0.1 M (circles), 0.2 M (squares), or 0.5 M (triangles). In each case the voltage dependence of the ratio *Iss/Io* from traces like those in Fig. 6*a* have been reported.

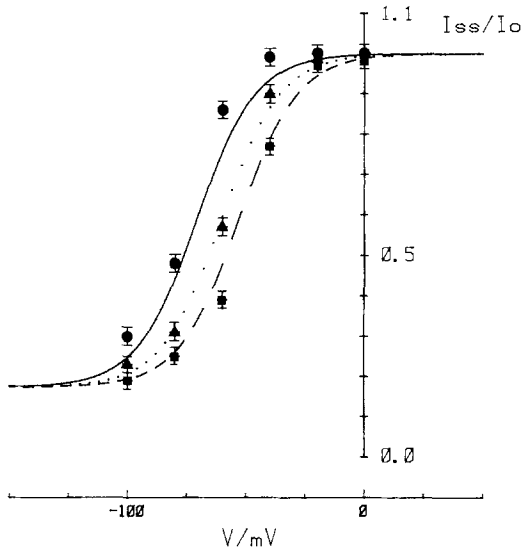

Fig. 8. Combined effects of voltage and Ca^{2+} concentration on the ratio *Iss/Io* under the same experimental conditions of Fig. 6. Ca^{2+} was added only to the *trans* compartment to a final concentration of 40 mM (circles), 60 mM (triangles) and 80 mM (squares). Solid lines are drawn according to the inactivation model described in the text, with the parameters listed in Table 2

shown in a digitized form in part *b* on a half logarithmic scale. This relaxation has not a single time constant but can be fitted adequately well with the sum of two purely exponential components with different time constants. Both these time constants depend on the applied voltage as evidenced in part *c*; at least the larger time constant has a well-defined bell shape, i.e. it goes through a maximum when the magnitude of the potential is increased.

The behavior shown in Fig. 6 for the case of Ca^{2+} is qualitatively quite general. We have used a number of polyvalent cations i.e. Mg^{2+}, Ba^{2+}, Zn^{2+} and Tb^{3+} and with all of them we have observed a voltage-dependent inhibition of the α-toxin induced conductance; the ratio *Iss/Io* is in general a sigmoidal function of the applied voltage; the current relaxations can always be described as the sum of two exponential components whose time constants are bell-shaped functions of the final voltage (*see* Fig. 11).

Symmetrical or asymmetrical addition of Ca^{2+} to the bathing solutions has markedly different effects. As Fig. 7 shows, the addition of Ca^{2+} only on the *cis* side inhibits the channel conductance mainly when positive potentials are applied. Conversely, the addition of Ca^{2+} only on the *trans* side has much stronger effects when negative potentials are applied. Finally, if Ca^{2+} is added on both sides, two voltage-dependent inactivation regions develop, one for positive and one for negative potentials. This behavior is almost independent of the KCl concentration, which is the main electrolyte present, at least in the range 0.1 to 0.5 M.

The effects of Ca^{2+} and the other polyvalent cations tested are strongly dose dependent, i.e. the higher the concentration of the inhibiting cation the higher is the reduction of the current at a given voltage. This is shown in detail for the case of Ca^{2+} in Fig. 8. Here the effects of three different concentrations of this cation, added to the *trans* solution, on the negative voltage branch of the current inactivation curve are presented. At any concentration the inactivation depends sigmoidally on the applied voltage; at any given voltage the inactivation is stronger the larger the concentration of Ca^{2+}.

The dose dependence of the ratio *Iss/Io* at the fixed voltage of −100 mV is reported in Fig. 9 for all the inhibiting cations we have tested. In any case the residual conductance decreases sigmoidally with the inhibitor concentration when this is reported on a logarithmic scale. The order of the effi-

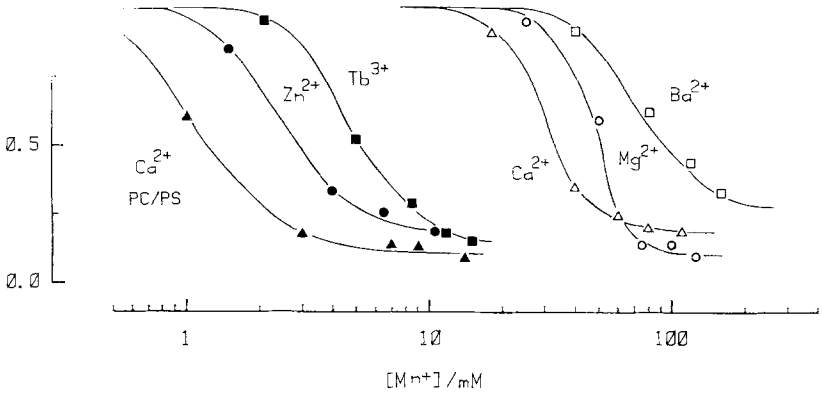

Fig. 9. Dose dependence of the inhibiting effects of polyvalent cations on the conductance induced by α-toxin in planar lipid membranes. The ratio *Iss/Io* at a fixed potential of −100 mV has been measured as a function of the concentration M^{n+} of di- and trivalent cations added either to the *trans* only or to both the 0.1 M KCl solutions bathing the membrane. The symbols □, ○, △, ■, ●, have been used for Ba^{2+}, Mg^{2+}, Ca^{2+}, Tb^{3+} and Zn^{2+}, respectively, on membranes comprised of egg PC. ▲ are for Ca^{2+} effects when negatively charged membranes comprised of a 1 : 1 PC : PS mixture are used. Solid lines are drawn by eye

ciency in inhibiting the α-toxin-induced conductance that we have found is: $Ba^{2+} < Mg^{2+} < Ca^{2+} < Tb^{3+} < Zn^{2+}$. We have also found that the inhibiting efficiency of these cations depends strongly on the membrane composition. In fact changing the bilayer from a pure PC one to a negatively charged PC/PS (1 : 1) film, increases the inhibiting efficiency of Ca^{2+} roughly by a factor of 30, as shown in Fig. 9. It is interesting at this point to go deeper inside the mechanics of inhibition. If we assume that a membrane contains a fixed number of α-toxin channels, say n, which in the presence of a polyvalent cation at steady state may be either open, with probability po and current io, or closed, with probability pc and current ic, then for a voltage jump like those in Fig. 6*a* we have:

$$Iss/Io = (po \cdot n \cdot io + pc \cdot n \cdot ic)/n \cdot io = po + pc(ic/io) \quad (1)$$

where we have assumed that at the initial instant all the channels were open. Introducing the parameter ic/io and remembering that $po + pc = 1$ we can rearrange the experimental points of Fig. 9 in a Hill plot reporting the ratio pc/po versus the inhibitor concentration on a double-logarithmic scale as shown in Fig. 10. It is found that straight lines can fit to the points in a Hill plot. The mean slope of these lines is 2.50 ± 0.25 which indicates that two to three cations are involved in the inhibition of the channel.

Finally we would like to mention that control experiments performed adding Ca^{2+} to the bathing solution before giving α-toxin to the membrane have shown that the divalent cation cannot prevent the formation of pores but produces also in this case a voltage-dependent block of the channels.

Discussion

General Features

It is now widely recognized that *S. aureus* α-toxin forms ion channels into the membranes of target cells through aggregation of hydrophilic monomers into an amphiphilic hexamer of molecular weight roughly 200 kD (7, 12, 19, 39]. Consistently with the hypothesis of pore formation we have observed the appearance of discrete steps in the current flowing through a voltage-clamped bilayer after the interaction with *S. aureus* α-toxin (Fig. 1). These conductance jumps are a strong indication that ionic channels are formed into the bilayer and indeed the incorporation patterns shown in Fig. 1 are quite similar to that observed with other well-known pore-forming proteins such as hemocyanin [29], porin [4] and colicin [15]. Consistently with the hypothesis of aggregate formation we have measured a power dependence of the pore-formation rate on the toxin aqueous concentration larger than one (G. Menestrina, *unpublished result*).

From the discrete steps, histograms of single-channel conductance have been constructed. These histograms, as shown in the insert of Fig. 1, are nonsymmetrical, presenting an excess of events at low conductance values for each KCl concentration. We think that these events, which represented in 25 experiments a fraction of 8.1 ± 1.3% of the

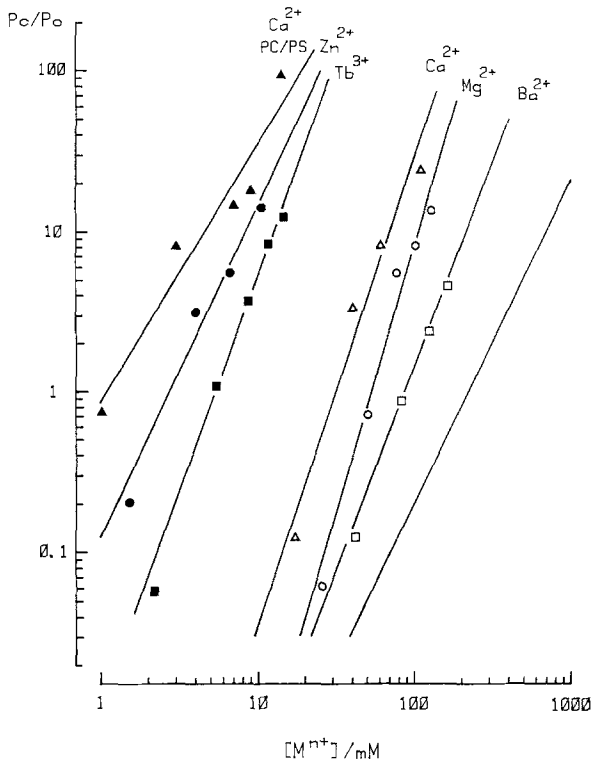

Fig. 10. Rearrangement of the experimental points of Fig. 9 in a Hill plot reporting the ratio between the probability of the channel of being closed *Pc* and that of being open *Po* as a function of the polyvalent cations concentration in a double-logarithmic plot. Symbols and experimental conditions are as in Fig. 9. Straight lines are least-squares fit whose slopes from left to right are: 1.6, 2.1, 2.7, 2.8, 3.3 and 2.5. A straight line of slope 2.0 is reported on the right side for comparison. The values of *ic*/*io* used are 0.07, 0.15, 0.12, 0.08, 0.16 and 0.23 in the same order as above. Apparent dissociation constants, i.e. the concentrations for equiprobability of the two configurations, are: $K(Ca^{2+})$ (in PC : PS membranes) = 1.2 mM; $K(Zn^{2+})$ = 3.2 mM; $K(Tb^{3+})$ = 6 mM; $K(Ca^{2+})$ = 28 mM; $K(Mg^{2+})$ = 54 mM and $K(Ba^{2+})$ = 88 mM; the last five values have been obtained with PC bilayers

total number of events, may be due to the formation of channels by aggregates containing less than 6 monomers. In particular a pentamer precursor of the hexamer has been observed recently in structural studies [39]. It is conceivable that if also a pentameric channel can be formed in the membrane this has a lower conductance than the hexameric one, its internal diameter being smaller, as is the case, for example, of the well-known pore formed by the antibiotic alamethicin [10, 22].

The linear dependence of the channel conductance on the solution conductivity, as shown in Fig. 2, suggests that these pores are large and filled with aqueous solution. If this is the case, and assuming a cylindrical shape, the conductance G of the pore can be expressed as:

$$G = (\pi r^2/l) \cdot \sigma \qquad (2)$$

where r and l are radius and length of the pore while σ is the conductivity of the solution. From Fig. 2 a best-fit value of $10.1 \pm 1.0 \times 10^{-9}$ cm is obtained for $R = G/\sigma$ which, after substitution into Eq. (2) gives a value of 5.7 ± 0.2 Å for r, if a value of 100 Å, which corresponds to the structural data [39], is used for the pore length l. From this simplistic model the pore diameter can thus be roughly estimated to be 11.4 ± 0.4 Å in good agreement with the finding that σ-toxin at lytic concentrations (20 μg/ml) releases sucrose (8.8 Å effective diameter) but not inulin (diameter 30 Å) from resealed erythrocyte ghosts [21] and that dextran 4 of mol wt 4000 (average diameter 10 to 12 Å) effectively protects cells from osmotic lysis induced by α-toxin when applied externally [6].

That the pore is not a simple hole filled with aqueous solution is shown by the nonohmic behavior of the current-voltage curve (Fig. 3) and by its slight anion selectivity (Table 1). These findings imply that at least in a region of the pore the transport of ions is restricted. The voltage dependence of the single-channel conductance (empty points of Fig. 3) further indicates that the channels are asymmetrically inserted into the bilayer. In fact, since the mean single-channel conductance, in 0.1 M KCl, is 60 pS at −80 mV and 96 pS at +80 mV and since no channel of conductance larger than 75 pS has been observed at −80 mV we can conclude that all the channels feel a transmembrane potential of the same sign, i.e. that they are oriented parallely in the membrane. Furthermore, the excellent agreement between the single-channel and the many-channel current-voltage curves, after proper normalization at +40 mV, indicates that all the channels in a bilayer act independently.

The reversal potential under asymmetrical solution conditions can be calculated using a very general expression [38]:

$$V_{rev} = \frac{kT}{e} \sum_i \frac{t_i}{z_i} \ln \frac{f_i c_i}{f_i' c_i'} \qquad (3)$$

where e is the charge of the electron, k and T have their usual meaning, z_i, c_i and f_i indicate, respectively, valence, concentration and activity coefficient of the ion species i whereby unprimed letters stand for the *cis* compartment and primed stand for the *trans*; finally t_i is the transference number for the ion species i, which is related to the channel conductance G by:

$$t_i = \frac{Gi}{G} \qquad (4)$$

where Gi is the partial ionic conductance of the species i. From the reversal potential measured in KCl

solutions we obtain a ratio t_{Cl^-}/t_{K^+} of 1.5 at pH 7.0 and of 2.3 at pH 5.0, indicating a slight anion selectivity which increases at low pH. Since α-toxin is a positively charged protein, with an isoelectric point $pI = 8.5$ [18], we can reasonably attribute its anion selectivity to the presence of positively charged groups near the ion pathway which attract anions and repel cations. This interpretation has the advantage of giving a straightforward explanation also to the increase of the selectivity at the lower pH since the number of positively charged groups is increased at low pH and hence also their effects on anions. A similar pH dependence of the ion selectivity has been found with other channel formers like hemocyanin [31], porin [3] and colicin E1 [37] and attributed also in those cases to the effects of charged groups of these proteins.

It is interesting to compare the α-toxin single-channel conductance measured in pure PC and mixed (1 : 1) PC : PS bilayers, in the presence of 0.1 M KCl. If the pore entrance is located near the membrane surface the local ion concentration should be completely different in the two cases due to the negative surface charge of the membranes containing the acidic lipid PS, which increases the local cation concentration and decreases the anion one. The surface potential of PC : PS membranes (molar ratio 1 : 1) in a 0.1 M KCl solution can be estimated from ref. [17] to be as large as −85.5 mV, producing a roughly 30-fold increase in the local concentration of the permeant cation K^+, whereas the mean channel conductance measured was $G(PC) = 88.1 \pm 1.6$ pS (mean ± SD of 17 experiments) and $G(PC/PS) = 79.2 \pm 2.0$ pS (in 11 experiments). The lack of effects of the surface potential on the single-channel conductance seems to suggest that the pore entrance is located far away from the surface of the membrane in agreement with the structural studies on this channel which have indicated that it protrudes from the plane of the membrane into the solution for about 40 Å [8].

Blocking Effects of Polyvalent Cations

As shown in Figs. 4 and 6, Ca^{2+} can inhibit the α-toxin-induced conductance in a voltage-dependent way. Before introducing a model which can account for these effects we would like to make some considerations upon which the model will lie.

Figure 5 clarifies that this inhibition is due to the appearance of voltage-dependent fluctuations of unitary size which may be reasonably attributed to transitions of the channels between one conducting configuration (channel open) and one nonconducting, or poorly conducting, configuration (channel closed). The size of these conductance fluctuations, roughly 160 pS in the experimental conditions of Fig. 5, is independent of voltage and exceeds the value which could be expected from the actual K^+ and Cl^- concentrations which may be estimated to be about 130 pS (using the linear relationship of Fig. 2 and the transference number ratio of 1.5 from Table 1), and hence strongly suggests that Ca^{2+} ions are themselves permeant through the channel, with a partial conductance $G_{Ca^{2+}}$ of about 30 pS at 40 mM. This has been directly confirmed in two ways: first, by measuring the reversal potential in a $CaCl_2$ gradient (*see* Table 1), which indicates that anion selectivity is only a little bit larger in the case of $CaCl_2$ than in the case of KCl; second, measuring the single-channel conductance in 50 mM $CaCl_2$ which is found to be 97 ± 3 pS giving a $G_{Ca^{2+}}$ of 34.5 ± 1.0 pS at 50 mM, in good agreement with the case of the mixed KCl + $CaCl_2$ solution.

Figure 7 indicates that the action of Ca^{2+} is asymmetrical, i.e. that Ca^{2+} on the *cis* side produces inhibition of the channels when positive voltages are applied and conversely Ca^{2+} on the *trans* side produces inhibition if negative transmembrane voltages are used. We think that the small effects seen at negative voltages when Ca^{2+} is present on the *cis* side can be due in fact to Ca^{2+} ions which arrive at the *trans* side diffusing through the channel, and conversely for the small effects at positive potentials when Ca^{2+} is added to the *trans* compartment.

Hence we assume, on the basis also of the dose-dependence curves shown in Fig. 9, the existence of at least one site for the specific binding of Ca^{2+} and the other polyvalent cations on the *trans* side, whose occupancy gives rise to the negative voltage inhibition, and one on the *cis* side for the positive potential inhibition. The two sites act independently and therefore may be treated independently.

The next consideration is that the voltage dependence cannot arise, as in many other cases described in the literature [14, 25, 41] from the sites inside the channel where they feel a part of the potential drop, since for example Ca^{2+} on the *trans* side inhibits the channels when negative potentials are applied on this side, i.e. potentials which drive positively charged ions out of the channel into the solution, whereas one would expect the opposite to occur for a voltage-dependent binding step.

Another possibility is that the effects of Ca^{2+} and the other polyvalent cations are due to their binding to the PC molecules comprising the membrane. We also think that this possibility is unlikely for at least two reasons: first the intrinsic binding constants which may be evaluated from Fig. 9 to be 14.3, 20 and 33.3 M^{-1} for Ba^{2+}, Mg^{2+} and Ca^{2+}, respectively, are quite larger than those which have been measured for PC molecules in planar bilayers by McLaughlin et al. [27], which are 3.6, 1 and 1 M^{-1} for the same cations and in the same order as above, and seem to follow an even different se-

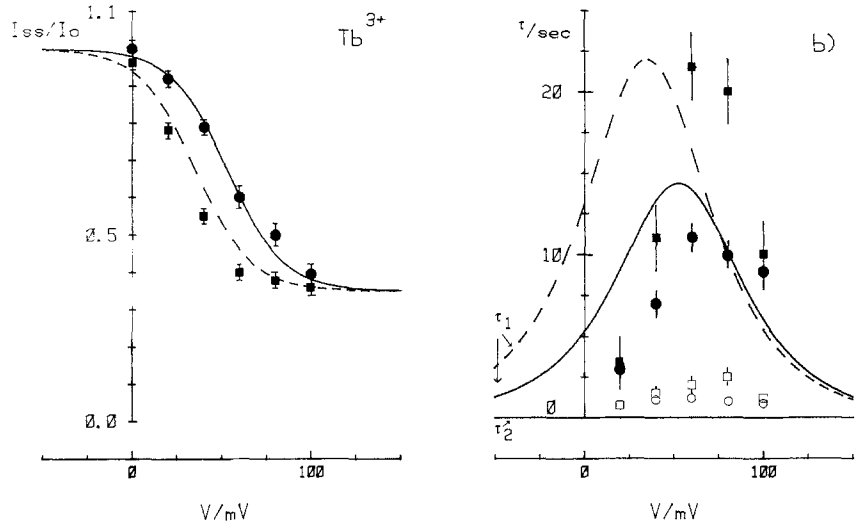

Fig. 11. Combined effects of voltage and inactivating cation concentration on the ratio *Iss/Io* and the two time constants τ_1 and τ_2 in experiments similar to those in Fig. 6 but in the presence of Tb^{3+}. Tb^{3+} was added to the *cis* side at the concentration of either 5 mM, circles and solid lines, or 9 mM, squares and dashed lines. Empty points are for the faster time constant τ_2. Theoretical lines are drawn according to the inactivation model described in the text with the fit parameters listed in Table 2

quence; second in the case of cation binding to PC molecules a continuous decrease in the channel conductance would be expected as progressively more PC molecules are titrated rather than an all-or-nothing effect as that shown in Fig. 5.

Hence we suggest that the sites are located on the outer faces of the channel and at a certain distance from the surface of the bilayer. An estimate of the distance of the *trans* site from the plane of the membrane can be obtained from the difference in the apparent binding constant of Ca^{2+} in the case of neutral PC bilayers and negatively charged PC : PS ones, which may be inferred from Fig. 9. The apparent binding constant K_{app} for the case of the protein bound to a charged surface, can be calculated from the intrinsic constant K_{int} by:

$$K_{app} = K_{int} \cdot \exp(-ze/kT \cdot \psi s) \qquad (5)$$

where z is the valence of the binding ion, +2 in the case of calcium, e, k and T have been defined above and ψs is the potential at the site. From Eq. (4) we expect that the apparent binding constant of Ca^{2+} ions on the channel increases when negatively charged membranes are used and this is what has been observed indeed (Fig. 9). Assuming no surface charge for PC bilayers, i.e., $K_{app}(PC) = K_{int}$, and from the observed shift in the Ca^{2+} concentration dependence in Fig. 9, a potential ψs of −39 mV can be calculated for the case of PC/PS membranes. The surface potential of PC/PS membranes of molar ratio 1 : 1 can be calculated from [17, 28] to be −74.5 mV in the presence of KCl 0.1 M plus 2 mM $CaCl_2$; we may conclude that the Ca^{2+} binding site does not feel the whole surface potential, i.e. that it is located a small distance apart from the membrane solution interface. This distance, again using ref. [17], may be roughly estimated to be 4 Å, a value which indicates that the Ca^{2+} binding site is relatively far from the pore entrance which is located about 40 Å from the lipid surface.

Finally, the Hill plot of the equilibrium constant *pc/po* between the two configurations, closed and open, suggests that two to three polyvalent cations are involved in the inactivation of one α-toxin channel. From these Hill plots it is possible to calculate the dissociation constants for the binding of the different cations on the channel. We have found that the efficiency in inactivating the channel follows the sequence $Zn^{2+} > Ca^{2+} > Mg^{2+} > Ba^{2+}$ which is the same as that observed by Pasternak et al. [35] for the inhibition of the effects of this toxin on natural cells. Furthermore, the stability constants which can be obtained for these four cations, i.e. 2.50, 1.55, 1.27, 1.02 (in the same order as above), are in the range and follow the same sequence as the stability constants of the complexes that these metals form with a number of organic acids (*see* Table 1 in ref. 40), suggesting that a carboxyl group of the protein is involved in their binding. The finding that Tb^{3+} inactivates the channel in a manner similar to Ca^{2+} but at lower concentrations ($pK(Tb^{3+}) = 2.22$ and $pK(Ca^{2+}) = 1.55$) is consistent with the fact that lanthanide cations are known to be good vicariants of calcium since they bind to the proteins on the same sites where Ca^{2+} binds with a higher affinity [26].

On these bases we now introduce a model for the action of the inhibiting cations on the channel.

The Inactivation Gating Model

We have drawn our model onto the very general one presented recently by Moczydlowsky and Latorre for the Ca^{2+}-activated K^+ channel [33]. There are indeed some peculiar similarities between the two channels since they both enter open-closed fluctuations only in the presence of divalent cations and they both give Hill plots for the open-closed equilibrium with slopes around two (in the range 1.7 to 2.5 for the Ca^{2+}-activated K^+ channel (*see* ref. 32), and 2.50 ± 0.25 for the α-toxin channel), the main difference being that the α-toxin channel is normally open in the absence of divalent cations and hence should be termed a polycation-inactivated channel.

For the sake of simplicity we assume that two cations can bind to the channel on each side since this is the minimum number which is compatible with all of our findings.

As shown in ref. 33 a channel with two configurations, open O and closed C, which can bind two metal cations M has six possible states which can be arranged in an 8-shaped general scheme (⊟) as follows:

$$\begin{array}{ccc} O & \rightleftharpoons & C \\ \Updownarrow & & \Updownarrow \\ O^{\cdot M} & \rightleftharpoons & C^{\cdot M} \\ \Updownarrow & & \Updownarrow \\ O^{M}_{\cdot M} & \rightleftharpoons & C^{M}_{\cdot M} \end{array}$$

We have found that also in the case of the α-toxin channel the sub-scheme ⌙ can best describe the voltage-time-concentration dependence of the equilibrium between the states. Neither scheme ⌜ nor scheme ⌞ can be used since the first is excluded by the fact that only rare fluctuations between O and C are observed in the absence of cations M (*see* Fig. 1), and the second by the fact that it predicts time constants for the relaxations, in voltage-jump experiments, which decrease monotonously while the concentration of M is increased, whereas under appropriate conditions we have observed the reverse to occur. Schemes with more than three segments, like ⊟⌙⊟, have been avoided since they seem unnecessarily complicated.

The ⌙ scheme can be written in a linear form as:

$$O \overset{K_1}{\rightleftharpoons} O^{\cdot M} \underset{\beta}{\overset{\alpha}{\rightleftharpoons}} C^{\cdot M} \overset{K_2}{\rightleftharpoons} C^{M}_{\cdot M}. \qquad (6)$$

Assuming, in a first approximation, a very fast

Table 2. Best fit parameters used to produce the theoretical lines in Figs. 6, 8 and 11 according to the inactivation model[a]

Cation	K_1/mM	K_2/mM	q/e	Vo/mV	a/Hz	b/Hz	F
Mg^{2+}	100	0.05	1.8	−145	0.95	50	0.13
Ca^{2+}	80	0.03	2.0	−145	0.54	40	0.17
Tb^{3+}	1	0.09	1.6	+109	0.26	50	0.35
Zn^{2+}	0.5	0.06	1.9	+120	0.02	20	0.20

$$O \overset{K_1}{\rightleftharpoons} O^{\cdot M} \underset{\beta}{\overset{\alpha'}{\rightleftharpoons}} C^{\cdot M} \overset{K_2}{\rightleftharpoons} C^{M}_{\cdot M}$$

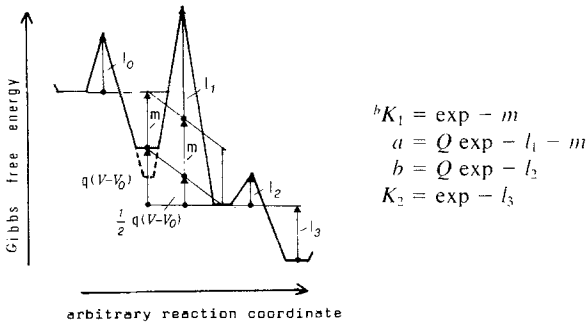

[b] $K_1 = \exp - m$
$a = Q \exp - l_1 - m$
$b = Q \exp - l_2$
$K_2 = \exp - l_3$

[a] K_1 and K_2 are the dissociation constants for the binding of the two inactivating cations to the open and closed channel, respectively. K_1 indicates a high selectivity of the channel, the sequence of affinities being: $Zn^{2+} > Tb^{3+} > Ca^{2+} > Mg^{2+}$, which agrees well with the values extrapolated from Fig. 10. K_2 is almost the same for all the cations and indicates a high affinity of the channel in the closed configuration for the binding of the second cation. q is the gating charge for the voltage-dependent process of channel closure, its mean value is 1.8 ± 0.1 electronic charges. Vo is a measure of the conformational energy difference between the open and closed configuration of the channel in the absence of an applied electrical field, the mean value of this energy is 9.5 ± 1.0 kT. a gives a measure of the energy barrier which has to be overcome by the channel to close, when the applied voltage is Vo. The values found indicate that this energy barrier is different when different cations are bound to the open channel. The following sequence holds: $Zn^{2+} > Tb^{3+} > Ca^{2+} > Mg^{2+}$. Together with the affinity sequence (*see* K_1 above) this gives a strong indication that the energy E of the ground state for the open channel with one inactivating ion bound, is largely different for the different cations, being lowest for Zn^{2+}. The following sequence holds: $E_{Zn2-} < E_{Tb3+} < E_{Ca2+} < E_{Mg2+}$, and is at the origin of both the affinity and the forward energy barrier sequences, since a deeper well in this state implies a smaller dissociation constant and a smaller forward rate in the gating step. b is the forward transition rate for the binding of the second inactivating cation to the closed channel and it seems to be almost independent from the chemical nature of the cation. Together with the finding that K_2 is also almost constant this indicates that the energetic of the last step is the same for every cation, and represents a high-affinity high-rate reaction. A sketch of the possible energy profile for the whole scheme (A1) is given at the bottom of the Table. The last parameter F indicates the ratio between closed and open channel conductance; the values found are in good agreement with those used to produce Fig. 10.
[b] The energies m and l_i (with $i = 0$ to 3) are given in kT units; Q is a frequency factor of statistical origin [9]. Only m is supposed to vary with the chemical nature of the binding cation.

equilibrium between O–$O^{\cdot M}$ and $C^{\cdot M}$–$C^{\cdot M}_{M}$ compared to the step $O^{\cdot M}$–$C^{\cdot M}$, one can calculate a single time constant for the relaxations of the system in voltage-jump experiments, which is [33]:

$$\tau = 1/(\alpha' + \beta') \tag{7}$$

with:

$$\alpha' = \alpha/(1 + K_1/M) \tag{8}$$

$$\beta' = \beta/(1 + M/K_2). \tag{9}$$

Combining Eqs. (7, 8 and 9) it is possible to show that τ increases either at very low M values, i.e. for $M \ll K_1, K_2$, or at very high M values, $M \gg K_1, K_2$, as we have experimentally observed to occur. The above assumptions are equivalent to treat the α-toxin channel as a two-state one; on the other hand we have observed the appearance of two time constants in the current relaxations and hence we have decided to release the assumption that the last step in scheme 6 is fast and to treat the α-toxin channel as a three-state one. Current relaxations which result from the sum of two exponential components with positive amplitudes are predicted by this model which are quite similar to those we have observed with the channel (Fig. 6).

The mathematical treatment of the model is given in the Appendix. It has been used to generate the lines in Figs. 6, 8 and 11 giving the parameters which are listed and discussed in Table 2. There is a good general agreement between the model predictions and the experimental findings except that for the second, faster time constant which always results in being too short to fit the experimental results. We think that it is not safe here to look for a more complicated model which could account also for those data, since more experiments at the single-channel level are needed which are now underway in our laboratory.

I would like to thank Prof. C. A. Pasternak for a kind discussion in Bucharest, Romania (Nov. 1984) which has originated the idea of this work and for subsequent encouragement and advice. I am also grateful to Prof. S. Bhakdi for numerous suggestions and comments on the manuscript. I am indebted to Dr. K. D. Hungerer of the Behringwerke Laboratories (Marburg D) for having provided me with samples of purified *S. aureus* α-toxin. This work has been financially supported by the Italian Ministero di Pubblica Istruzione and Consiglio Nazionale delle Ricerche.

References

1. Arbuthnott, J.P., Freer, J.H., Billcliffe, B. 1973. Lipid-induced polymerization of staphylococcal α-toxin. *J. Gen. Microbiol.* **75**:309–319
2. Bashford, C.L., Alder, G.M., Patel, K., Pasternak, C.A. 1984. Common action of certain viruses, toxins and activated complement: Pore formation and its prevention by extracellular Ca^{2+}. *Biosci. Rep.* **4**:797–805
3. Benz, R., Darveau, R.P., Hancock, R.E.W. 1984. Outer membrane protein PhoE from *Escherichia coli* forms anion selective pores in lipid-bilayer membranes. *Eur. J. Biochem.* **140**:319–324
4. Benz, R., Ishii, J., Nakae, T. 1980. Determination of ion permeability through the channels made of porins from the outer membrane of *Salmonella typhimurium* in lipid bilayer membranes. *J. Membrane Biol.* **56**:19–29
5. Bhakdi, S., Füssle, R., Tranum-Jensen, J. 1981. Staphylococcal α-toxin: Oligomerization of hydrophilic monomers to form amphiphilic hexamers induced through contact with deoxycholate detergent micelles. *Proc. Natl. Acad. Sci. USA* **78**:5475–5479
6. Bhakdi, S., Muhly, M., Füssle, R. 1984. Correlation between toxin binding and hemolytic activity in membrane damage by staphylococcal alpha-toxin. *Infect. Immunol.* **46**:318–323
7. Bhakdi, S., Tranum-Jensen, J. 1983. Membrane damage by channel-forming proteins. *Trends Biochem. Sci.* **8**:134–136
8. Bhakdi, S., Tranum-Jensen, J. 1984. Mechanism of complement cytolysis and the concept of channel-forming proteins. *Philos. Trans. R. Soc. London B.* **306**:311–324
9. Bockris, J.O.M., Reddy, A.K.N. 1970. Modern Electrochemistry. Vol. 1. Plenum, New York
10. Boheim, G., Kolb, H.-A. 1978. Analysis of the multi-pore system of alamethicin in a lipid membrane. I. Voltage-jump current-relaxation measurements. *J. Membrane Biol.* **38**:99–150
11. Bukelew, A.R., Colacicco, G. 1971. Lipid monolayers. Interaction with staphylococcal α-toxin. *Biochim. Biophys. Acta* **233**:7–16
12. Cassidy, P., Six, A.R., Harshmann, S. 1974. Biological properties of Staphylococcal α-toxin. *Biochim. Biophys. Acta* **332**:413–425
13. Colquohun, D., Hawkes, A.G. 1977. Relaxation and fluctuations of membrane currents that flow through drug-operated ion channels. *Proc. R. Soc. London* **199**:231–262
14. Coronado, R., Miller, C. 1979. Voltage-dependent caesium blockade of a cation channel from fragmented sarcoplasmic reticulum. *Nature (London)* **280**:807–810
15. Davidson, V.L., Brunden, K.R., Cramer, W.A., Cohen, F.S. 1984. Studies on the mechanism of action of channel-forming colicins using artificial membranes. *J. Membrane Biol.* **79**:105–118
16. Ehrenstein, G., Lecar, H. 1977. Electrically gated ionic channels in lipid bilayers. *Q. Rev. Biophys.* **10**:1–34
17. Eisenberg, M., Gresalfi, T., Riccio, T., McLaughlin, S. 1979. Adsorption of monovalent cations to bilayer membranes containing negative phospholipids. *Biochemistry* **18**:5213–5223
18. Freer, J.H. 1982. Cytolytic toxins and surface activity. *Toxicon* **20**:217–221
19. Freer, J.H., Arbuthnott, J.P., Bernheimer, A.W. 1968. Interaction of staphylococcal α-toxin with artificial and natural membranes. *J. Bacteriol.* **95**:1153–1168
20. Freer, J.H., Arbuthnott, J.P., Bilcliffe, B. 1973. Effects of staphylococcal α-toxin on the structure of erythrocytes membranes. *J. Gen. Microbiol.* **75**:321–332
21. Füssle, R., Bhakdi, S., Sziegoleit, A., Tranum-Jensen, J., Kranz, T., Wellensiek, H.J. 1981. On the mechanism of

membrane damage by *Staphylococcus aureus* α-toxin. *J. Cell Biol.* **91:**83–94
22. Gordon, L.G.M., Haydon, D.A. 1975. Potential dependent conductances in lipid membranes containing alamethicin. *Philos. Trans. R. Soc. London B.* **270:**433–447
23. Harshman, S. 1979. Action of staphylococcal α-toxin on membranes: Some recent advances. *Mol. Cell. Biochem.* **23:**142–152
24. Harshman, S., Sugg, N. 1985. Effect of calcium ions on staphylococcal alpha-toxin induced hemolysis of rabbit erythrocytes. *Infect. Immunol.* **47:**37–40
25. Lee, K.S., Akaike, N., Brown, A.M. 1978. Properties of internally perfused, voltage-clamped, isolated nerve cell bodies. *J. Gen. Physiol.* **71:**489–507
26. Martin, R.B., Richardson, F.S. 1979. Lanthanides as probes for calcium in biological systems. *Q. Rev. Biophys.* **12:**181–209
27. McLaughlin, A., Grathwohl, C., McLaughlin, S. 1978. The adsorption of divalent cations to phosphatidylcholine bilayer membranes. *Biochim. Biophys. Acta* **513:**338–357
28. McLaughlin, S., Mulrine, N., Gresalfi, T., Vaio, G., McLaughlin, A. 1981. Adsorption of divalent cations to bilayer membranes containing phosphatidylserine. *J. Gen. Physiol.* **77:**445–473
29. Menestrina, G., Antolini, R. 1981. Ion transport through hemocyanin channels in oxidized cholesterol artificial bilayer membranes. *Biochim. Biophys. Acta* **643:**616–625
30. Menestrina, G., Maniacco, D., Antolini, R. 1983. A kinetic study of the opening and closing properties of the hemocyanin channel in artificial lipid bilayer membranes. *J. Membrane Biol.* **71:**173–182
31. Menestrina, G., Porcelluzzi, C. 1985. Dependence of ion flow through the hemocyanin channel on a fixed charge at the pore mouth: Effects of H^- and Ca^{2+} ions. *Biochim. Biophys. Acta (in press)*
32. Methfessl, C., Boheim, G. 1982. The gating of single Ca^{2+}-dependent K^+ channels is described by an activation/blockade mechanism. *Biophys. Struct. Mech.* **9:**35–60
33. Moczydlowski, E., Latorre, R. 1985. Gating kinetics of Ca^{2+} activated K^+ channels from rat muscle incorporated into planar lipid bilayers. *J. Gen. Physiol.* **82:**511–542
34. Montal, M., Mueller, P. 1972. Formation of bimolecular membranes from lipid monolayers and a study of their electrical properties. *Proc. Natl. Acad. Sci USA* **69:**3561–3566
35. Pasternak, C.A., Bashford, C.L., Micklem, K.J. 1985. Ca^{2+} and the interaction of pore formers with membranes. *J. Biosci.* **8:**273–291
36. Pitzer, K.S. 1979. Theory: Ion interaction approach. *In:* Activity Coefficients in Electrolyte Solutions. R.M. Pytkovicz, editor. Vol. 1, pp. 158–208. CRC Press, Boca Raton, Florida
37. Raymond, L., Slatin, S.L., Finkelstein, A. 1985. Channels formed by Colicin E1 in planar lipid bilayers are large and exhibit pH-dependent ion selectivity. *J. Membrane Biol.* **84:**173–181
38. Schultz, S.G. 1980. Basic Principles of Membrane Transport. Cambridge University Press, New York
39. Tobkes, N., Wallace, B. A., Bayley, H. 1985. Secondary structure and assembly mechanism of an oligomeric channel protein. *Biochemistry* **24:**1915–1920
40. Williams, R.J.P. 1952. The stability of complexes of the group IIA metal ions. *J. Chem. Soc.* 3770–3778
41. Woodhull, A.M. 1973. Ionic blockage of sodium channels in nerve. *J. Gen. Physiol.* **61:**687–708

Received 24 September 1985; revised 3 December 1985

Appendix

We have decided to use the following scheme as a working hypothesis for the α-toxin channel gating inactivation pathway:

$$O \overset{K_1}{\rightleftharpoons} O^{\cdot M} \underset{\beta}{\overset{\alpha'}{\rightleftharpoons}} C^{\cdot M} \overset{K_2}{\rightleftharpoons} C^M_M. \tag{A1}$$

where K_1 and K_2 are the dissociation constants for the two steps involving the binding of the cation M, whereas α' and β are the forward and backward transition rates for the closing reaction and can be written, according to a general two-state voltage-gating mechanism [16], in the following way:

$$\alpha' = a \exp \frac{q \cdot (V - Vo)}{2kT} \tag{A2}$$

$$\beta = a \exp \frac{-q \cdot (V - Vo)}{2kT} \tag{A3}$$

where q is the gating charge and $q \cdot Vo$ the conformational energy difference between the two states, open and closed.

Since the binding sites are supposed to be located outside the ion pathway (*see* text), we assume here that all of the voltage dependence resides in the voltage-gating step, i.e. in the two transition rates, α' and β. For the rest we assume also that the two open states have equal conductance and so also the two closed states.

If we suppose that the first reaction is in fast equilibrium compared to the others we can simplify scheme (A1) into a pseudo 3-states model as follows [32]:

state 1 2 3

$$O^{\cdot M} \underset{\beta}{\overset{\alpha}{\rightleftharpoons}} C^{\cdot M} \underset{\delta}{\overset{\gamma}{\rightleftharpoons}} C^M_M \tag{A4}$$

where:

$$\alpha = \alpha'/(1 + K_1/M) \tag{A5}$$

$$\gamma = b \cdot M \tag{A6}$$

$$\delta = b_{-1} \tag{A7}$$

and the relation

$$K_2 = b_{-1}/b \tag{A8}$$

holds.

We now define $\bar{x}(t)$ as a column vector whose entries are the occupancies of the three states at time t (sum of the entries = 1), which we call the state vector. The time dependence of the state vector can be appropriately described by means of a matrix $\bar{B}$ containing the transition rates which is defined as follows [30]:

$$\bar{B} = \begin{pmatrix} -\alpha & \beta & O \\ \alpha & -(\beta + \gamma) & \delta \\ O & \gamma & -\delta \end{pmatrix} \tag{A9}$$

The time evolution of the system from the initial state $\bar{x}(o)$ is in fact given by [13]:

$$\bar{x}(t) = e^{\bar{B}t}\bar{x}(o). \tag{A10}$$

The conductance of the membrane at time t, $G(t)$, can be calculated as n times the scalar product of the state vector with the conductance vector (a row vector whose entries are the conductances of each state):

$$G(t) = n\bar{G} \cdot \bar{x}(t) \tag{A11}$$

where n is the number of channels, supposed to be all equal, present in the membrane.

Using:

$$\bar{G} = Go(\ 1\ F\ F\ ) \tag{A12}$$

where Go is the conductance of the channel in either of the two open states, whereas that in the closed states is $Gc = F \cdot Go$ and

$$\bar{x}(o) = \begin{pmatrix} 1 \\ 0 \\ 0 \end{pmatrix} \tag{A13}$$

which corresponds to having all the channels in the open state at the time of the transition (what has been obtained clamping the membrane at 0 mV for a sufficient time before jumping the voltage), then, by standard treatment of Eq. (A10) [13] we have:

$$\frac{I(t)}{I(o)} = \frac{G(t)}{G(o)} = A(0) + A(1)\exp\lambda(1)t + A(2)\exp\lambda(2)t \tag{A14}$$

where $\lambda(1)$ and $\lambda(2)$ are the nonzero eigenvalues of the singular matrix $\bar{B}$, which are given by:

$$\lambda(1),\lambda(2) = \frac{-(\alpha + \beta + \gamma + \delta) \pm \sqrt{(\alpha + \beta - \gamma - \delta)^2 + 4\beta\delta}}{2} \tag{A15}$$

and both are negative.

The $A(i)$ terms are given by:

$$A(0) = \frac{\beta\delta + F(\alpha\delta + \alpha\gamma)}{\alpha\delta + \alpha\gamma + \beta\delta} \tag{A16}$$

$$A(1) = \frac{\alpha((\alpha + \beta + \lambda(2))(1 - F))}{\lambda(1)(\lambda(1) - \lambda(2))} \tag{A17}$$

$$A(2) = \frac{\alpha((\alpha + \beta + \lambda(1))(1 - F))}{\lambda(2)(\lambda(2) - \lambda(1))} \tag{A18}$$

and all are positive.

It follows from Eq. (A14) that the quantities reported in Figs. 6, 8 and 11 of this work are given by:

$$Iss/Io = A(0) \tag{A19}$$

$$\tau_1 = (\lambda(1))^{-1} \tag{A20}$$

$$\tau_2 = (\lambda(2))^{-2} \tag{A21}$$

where $\lambda(1)$ is obtained taking the plus sign in Eq. (A15).